Forces and Parameters of Permanent Magnet Linear Synchronous Machines

Z. DENG, I. BOLDEA, SENIOR MEMBER, IEEE, AND S. A. NASAR, FELLOW, IEEE

Abstract—**The determination of electromagnetic forces and parameters of permanent magnetic linear synchronous machines (PMLSM's), based on an evaluation of electromagnetic fields, as reported earlier, is considered. Analytical techniques applied to permanent magnet rotary synchronous machines are modified and adapted to PMLSM's. Fields were determined analytically in a single-sided PMLSM and computed results by the finite-element method were compared with those obtained experimentally in an earlier paper. A good correlation between the results were obtained by three procedures—analytical, finite-element computational method, and experimental. From these field evaluations the PMLSM parameters and performance are obtained.**

I. Introduction

PERMANENT MAGNET linear synchronous motors (PMLSM's) are proposed for numerous applications as summarized in [1]–[4]. As pointed out in an earlier paper [1], PMLSM's have certain unique features such as large airgaps, open-wide slots, pole and interpole configurations, flat or tubular structures, and existence of normal forces in flat PMLSM's. Consequently, standard formulas for rotary permanent magnet synchronous machines are not directly applicable to PMLSM's. The parameters, forces, and performance characteristics of PMLSM's must, therefore, be obtained from a detailed analysis and computation of the airgap electromagnetic fields. In the previous paper [1] we developed analytical expressions for the field distributions in a laboratory model flat single-sided PMLSM. In the present paper we utilize the previous results to obtain the machine constants from which we determine some of the machine performance characteristics. These computed results are then compared with those obtained experimentally to validate the assumptions made in deriving the mathematical model.

II. Machine Constants

In order to determine the machine constants we first obtain the voltage induced in the armature as follows, where we reconsider the flat PMLSM discussed in [1].

No Load Induced Voltage E_1

The voltage E_1 induced by the permanent magnet (PM) in the armature winding is given by

$$E_1 = \frac{\omega}{\sqrt{2}} W k_{w1} \tau L_A \frac{2}{\pi} (B_{yoI})_{\text{av}} \tag{1}$$

where $(B_{yoI})_{\text{av}}$ is the average flux density produced only by the PM in the phase winding of the armature. This average flux density is obtained from

$$(B_{yoI})_{\text{av}} = \frac{1}{h_w} \int_{h_t - h_w}^{h_t} B_{IPM}(y)\, dy \tag{2}$$

where

$$B_{IPM}(y) = \frac{1}{h_m} \int_0^{h_m} [B(y, y_m)]_I \, dy_m,$$

$$h_m + g_o \leqq y \leqq h_t \tag{3}$$

as given by [1, eq. (37)], with $A_{ls} = 0$ for no-load condition and h_m is the height of the magnet. A machine model with dimensions and the xy-axes is shown in Fig. 1. The important symbols in Fig. 1 are as follows: y_s is the arbitrary position of the primary current sheet along the actual slot height; y_m is the position of an equivalent current sheet which models the permanent magnet; and y_s varies from zero to the slot height h_s, whereas y_m varies from zero to the magnet height h_m. The results are finally averaged to better approximate the actual field distributions. Having obtained the no-load induced voltage, we proceed to determine the machine constants.

Machine Reactances

The longitudinal reactance X_{sd} is obtained from the induced voltage V_d as given by the following two equations:

$$V_d = X_{sd} I_s \tag{4}$$

where

$$V_d = \frac{\omega}{\sqrt{2}} W K_{w1} \tau L_A \frac{2}{\pi} (B_{yAI})_{\text{av}} \tag{5}$$

and $(B_{yAI})_{\text{av}}$ is the average flux density over the stator slot height produced by the stator current sheet only. Furthermore,

$$(B_{yAI})_{\text{av}} = \frac{1}{h_w^2} \int_{h_t - h_w}^{h_t} \left[\int_{h_t - h_w}^{h_t - y} B_{yI''}(y, y_s)\, dy_s + \int_{h_t - y}^{h_t} B_{yI'}(y, y_s)\, dy_s \right] dy \tag{6}$$

Manuscript received December 13, 1985; revised July 3, 1986. This work was supported by the National Science Foundation under Grants ECS-8314238 and INT-8408315.

Z. Deng and S. A. Nasar are with the Department of Electrical Engineering, University of Kentucky, Lexington, KY 40506.

I. Boldea is with the Department of Electrical Engineering, Polytechnical Institute, Timisoara, Romania.

IEEE Log Number 8611316.

where

$$B_{yI'} = j\sqrt{\mu_{xs}\mu_{ys}}\, H_{x1'} \left[\cosh K_s\left(y - (h_t - h_s)\right) + D \sinh K_s\left(y - (h_t - h_s)\right)\right] \quad (7)$$

$$B_{yI''} = j\sqrt{\mu_{xs}\mu_{ys}}\, H_{x1''} \left[\cosh K_s\left(y - h_t\right) + E \sinh K_s\left(y - h_t\right)\right] \quad (8)$$

which are obtained from [1, eqs. (23) and (25)] (with $A_{1m} = 0$). The stator slot leakage is already included in the above, but the end connection leakage is considered separately as follows. Notice that E_1 is given by (1) and (2) and X_{sd} is obtained from (4) and (5). It must be mentioned here that the desired expressions obtainable from (6)–(8) are much too cumbersome to express in a closed analytical form, primarily because of the expressions for the constants of integrations evaluated in [1]. Therefore, in general, it is advantageous to evaluate the integrals numerically, where the integration constant $E = 0$ in (8) and the constant D determined by solving the linear system of equations with eight unknowns obtained from [1, eqs. (28)–(35)].

End-Connection Leakage Reactance

Following the procedure in [5], for a flat structure with diamond-shaped coils, we obtain the following expression for the end-connection leakage reactance after making a few minor changes. This reactance X_e in the final form becomes

$$X_e = \frac{0.25mfW^2D_1k_{d1}^2}{p^3 \times 10^7}\left[\tan\alpha\left(\frac{\beta\pi - \sin\beta\pi}{\pi}\right) + 4.06\,K_{p1}^2\left(\ln\frac{4D_1}{r_1} - 1.75\right)\right]$$

where

$$D_1 = \frac{2\tau p}{\pi}\ (\text{inch}) \quad (9)$$

$$r_1 = h_{s/2}\ (\text{inch}) \quad (10)$$

k_{d1} = distribution factor

k_{p1} = pitch factor

β = ratio of coil span to pole pitch (see Fig. 2)

w_s = slot width

w_t = tooth width

C = coil end clearance

$$\sin\alpha = \frac{w_s + C}{w_s + w_t} \quad (11)$$

X_e is in ohms per phase per pole.

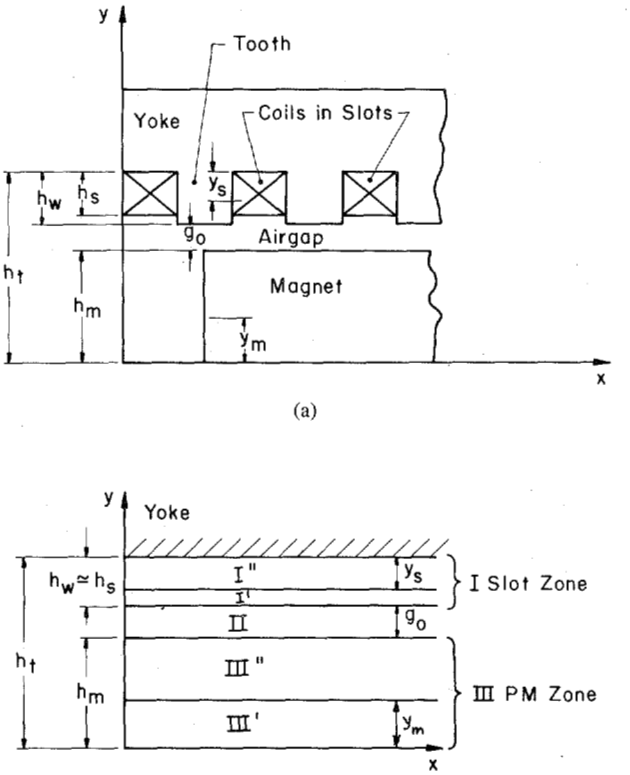

Fig. 1. (a) Longitudinal view of motor geometry. (b) General mathematical model.

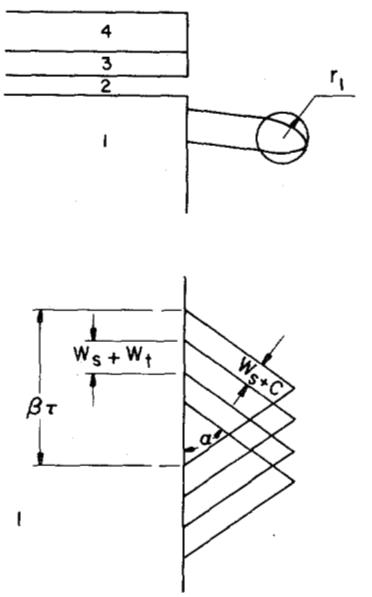

Fig. 2. Simplified model for calculation of end-connection leakage reactance. 1: Stator. 2: Airgap. 3: Permanent Magnet. 4: Back iron.

Hence the total longitudinal axis reactance of the machine X_s becomes

$$X_s = X_{sd} + X_e. \quad (12)$$

III. Determination of Forces

Because we are considering a single-sided PMLSM, in addition to the thrust F_x, a normal force F_n—of attraction type—is also developed between the primary and secondary cores.

In principle both these forces may be calculated either from the magnetic field distribution in the air gap or from the *dq-dq* model of the machine. It is simpler to calculate the forces from the *dq-dq* model equations by the power balance procedure.

The *dq-dq* model equations are

$$V_d = i_d R + \frac{d\psi_d}{dt} - \omega\psi_q \tag{13}$$

$$V_q = i_q R + \frac{d\psi_q}{dt} + \omega\psi_d \tag{14}$$

with

$$\psi_d = L_d i_d + M_{af} i_f = \text{flux linkage in the } d\text{-axis} \tag{15}$$

$$\psi_q = L_q i_q = \text{flux linkage in the } q\text{-axis.} \tag{16}$$

The thrust is obtained from the power balance by multiplying (13) by i_d and (14) by i_q. Consequently, we have

$$V_d i_d + V_q i_q = i_d^2 R + i_q^2 R + i_d \frac{d\psi_d}{dt} + i_q \frac{d\psi_q}{dt} + \omega(\psi_d i_q - \psi_q i_d). \tag{17}$$

The last term accounts for the mechanical power

$$F_x = \frac{\omega}{2\tau f}(\psi_d i_q - \psi_q i_d) = \frac{\pi}{\tau}(\psi_d i_q - \psi_q i_d). \tag{18}$$

The third and fourth terms in (17) may be expanded by differentiating with respect to the air gap g_0 to get the mechanical power due to the vertical motion (attraction force). We rewrite the complete form of (17) below:

$$V_d i_d + V_q i_q = i_d^2 R + i_q^2 R + \left(i_d \frac{\partial\psi_d}{\partial g_0} + i_q \frac{\partial\psi_q}{\partial g_0}\right)\dot{g}_0 + i_d \frac{\partial\psi_d}{\partial t} + i_q \frac{\partial\psi_q}{\partial t} + \omega(\psi_d i_q - \psi_q i_d). \tag{19}$$

Now the term multiplying $\dot{g}_0$ is the normal force. Hence,

$$F_n = i_d \frac{\partial\psi_d}{\partial g_0} + i_q \frac{\partial\psi_q}{\partial g_0}. \tag{20}$$

The relationship between the model and the three phase original motor parameters, currents, and voltages, are given by the Park Transformation. Hence,

$$M_{af} = \sqrt{\frac{3}{2}} \frac{E_1}{\omega I_f} = \sqrt{\frac{3}{2}} M'_{af} \tag{21}$$

where M'_{af} is the original inductance of the motor, and

$$I_f = H_c h_m \tag{22}$$

where E_1 has been previously determined, I_f is a fictitious equivalent current of the PM corresponding to its coercive force and height, and M_{af} is mutual inductance between the armature and the field. Furthermore current transformation yield

$$i_q = \sqrt{\frac{2}{3}}\left[i_a \sin\theta + i_b \sin\left(\theta - \frac{2\pi}{3}\right) + i_c \sin\left(\theta + \frac{2\pi}{3}\right)\right] \tag{23}$$

with $\theta = \omega t + \gamma_0$ and armature currents given by

$$i_a = \sqrt{2}\, I_s \cos\omega t$$

$$i_b = \sqrt{2}\, I_s \cos\left(\omega t - \frac{2\pi}{3}\right)$$

$$i_c = \sqrt{2}\, I_s \cos\left(\omega t + \frac{2\pi}{3}\right). \tag{24}$$

From (23) we obtain

$$i_q = \sqrt{3}\, I_s \sin\gamma_0 \tag{25}$$

From (18), we finally get the expression for the thrust as

$$F_x = \frac{\pi}{\tau}(\psi_d i_d - \psi_q i_d) = \frac{\pi}{\tau}\left[\sqrt{\frac{3}{2}} M_{af} I_f i_q + (L_d - L_q) i_d i_q\right]. \tag{26}$$

Since $L_d = L_q$ for the flat construction, (26) reduces to

$$F_x = \sqrt{\frac{3}{2}} \frac{\pi}{\tau} M_{af} I_f i_q. \tag{27}$$

For more than two poles

$$F_x = P\sqrt{\frac{3}{2}} \frac{\pi}{\tau} M_{af} I_f i_q \tag{28}$$

where P is the number of pole pairs.

IV. Numerical Example and Test Results

We obtained no load induced voltage E_1 from the amplitudes of the flux densities measured and calculated. The results are shown in Table I. The synchronous reactance

TABLE I

	Measured	Calculated by Finite Element Method	Calculated by Analytical Method
$E_{1(V)}$	334.2	327.4	376

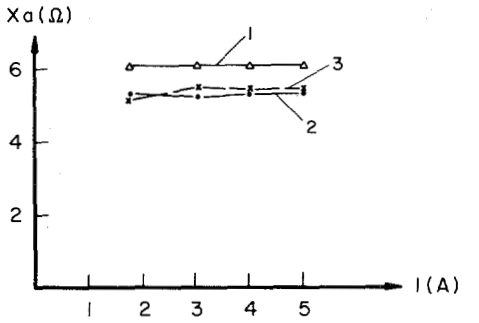

Fig. 3. X_a armature reaction reactance per pole in region covered by mover versus phase current. 1: X_a calculated by analytical method. 2: X_a calculated by finite-element method. 3: Measured X_a.

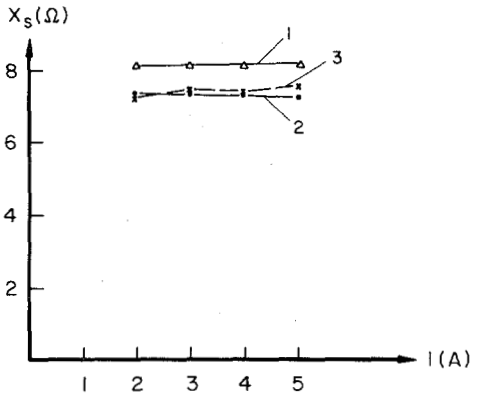

Fig. 4. X_s synchronous reactance per pole in region covered by mover versus phase current. 1: X_s calculated by analytical method. 2: X_s calculated by finite-element method. 3: Measured X_s.

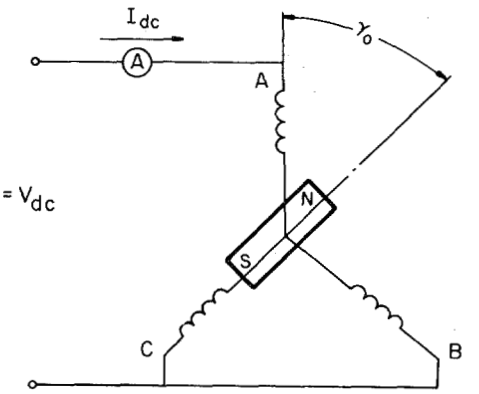

Fig. 5. Circuit for measuring forces.

Thrust Calculated

degree / I	30°		60°		90°		120°	
	FLM	AM	FLM	AM	FLM	AM	FLM	AM
4.95	11.5	11.3	19.9	19.6	23.0	22.6	19.9	19.6
6.36	14.8	14.5	25.6	25.2	29.6	29.1	25.6	25.2
8.00	18.6	18.3	32.2	31.7	37.2	36.6	32.2	31.7
9.48	22.05	21.7	38.2	37.6	44.1	43.4	38.2	37.6

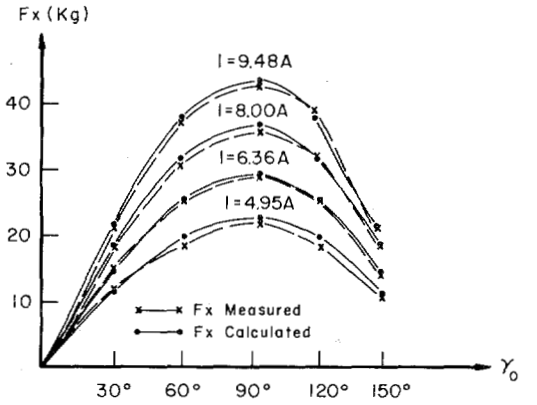

Fig. 6. Thrust versus γ_0.

for the flat PMLSM of [1] was calculated and then measured by *volt–ampere* standstill tests. The results for different values of stator phase currents are given in Figs. 3 and 4.

Standstill tests were conducted with the machine at rest. First, a laminated plate which was of the same size as the back iron of the mover was put above the stator and the distance between the stator and the laminated plate was maintained as equal to the sum of the height h_m of PM and the length g_0 of the air gap. A search coil of span equal to the pole pitch was located in the air gap. When armature was excited by a three phase source, the induced voltage in the search coil was measured. The armature reaction flux ϕ_a per pole, was calculated from the following expression:

$$E_c = 4.44\, f W_c \phi_a \qquad (29)$$

where E_c and W_c are, respectively, the induced voltage and the number of turns in the coil. Thus X_a, the armature reaction reactance per pole in the region covered by the mover, was obtained.

In order to measure the slot-leakage reactance and end-connection reactance, the mover was removed. With three phase excitation the reactance was measured. The reactance thus measured included: 1) slot-leakage reactance, 2) end-connection leakage reactance, 3) the reactance induced by fundamental component of the field, 4) tooth-top and zigzag leakage reactance, and 5) belt-leakage reactance. In most synchronous machines the last two reactances are a small portion of the total leakage reactance. So, these two reactances were neglected. A search coil was used again to determine the reactance X_f caused by fundamental field. If X_f is subtracted from the measured reactance X when the mover was removed, the sum of the slot-leakage reactance X_{sl} and end-connection reactance

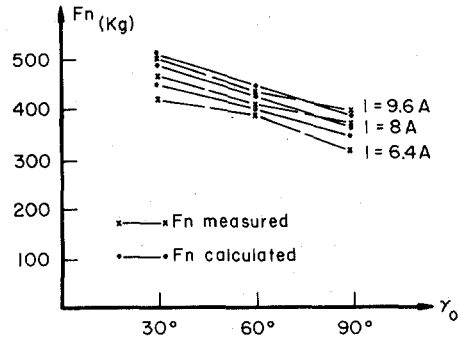

Fig. 7. Normal force versus γ_0.

X_e are obtained. Hence

$$X_{sl} + X_e = X - X_f. \tag{30}$$

Finally, we obtain the synchronous reactance as

$$X_s = X_a + X_{sl} + X_e. \tag{31}$$

Using strain gauges, thrust and normal forces were measured at standstill as functions of γ_0, which is the electrical angle between three phase resultant fundamental field and the fundamental field of the mover as shown in Figs. 5–7 for a few dc current values. The agreement between theory and experiments is considered satisfactory for design purposes.

V. Conclusion

Using the results of a previous paper, expressions for the parameters and forces of a flat PMLSM are derived. Analytical results are compared with those obtained by finite-element method and from tests. The agreement between the analytical model, finite-element model, and test results is considered acceptable for design and performance calculations of flat PMLSM's.

Nomenclature

$\overline{A}$	Instantaneous current sheet (A/m).
B	Magnetic flux density.
E	Electric field strength.
E_1	No load induced voltage.
f	Frequency.
h_m	Magnet height.
H	Magnetic field strength.
H_c	Coercive force of permanent magnet.
h_s	Slot height.
h_w	Height of conductors in a slot.
I_s	Stator phase current (RMS).
I_f	Fictitious equivalent current of permanent magnet.
i	Instantaneous current.
K_{d1}	Distribution factor.
K_{p1}	Pitch factor.
K_{w1}	Winding factor.
L_A	Width of the stator or mover.
L	Inductance.
m	Number of phases.
M	MMF.
P	Number of pole pairs.
t	Time.
τ_p	Magnet width.
τ_s	Slot pitch.
τ	Pole pitch.
W	Number of turns in series/phase.
x, y, z	Rectangular coordinates.
X	Reactance.
μ_r	Relative permeability of stator iron.
ϕ_a	Armature reaction flux per pole.
ψ	Magnetic flux linkage.
γ_0	Electrical angle between three phase resultant fundamental field and the fundamental field of the mover.

References

[1] Z. Deng, I. Boldea, and S. A. Nasar, "Fields in permanent magnet linear synchronous machines," *IEEE Trans. Magn.*, vol. MAG-22, no. 3, pp. 107–112, Mar. 1986.

[2] N. Boules and H. Weh, "Machine constants and design consideration for a high power, high speed permanent magnet disc type synchronous machine," *EME*, vol. 5, pp. 113–120, 1980.

[3] H. Weh and M. Shalaby, "Magnetic levitation with controlled permanentic excitation, *IEEE Trans. Magn.*, vol. MAG-13, no. 5, pp. 1409–1411, Sep. 1977.

[4] H. Weh, H. Mosebach, and H. May, "Design concepts and force generation in inverter-fed synchronous machine with permanent magnet excitation,"*IEEE Trans. Magn*, vol. MAG-20, no. 5, pp. 1756–1761, Sep. 1984.

[5] P. L. Alger, *The Nature of Polyphase Induction Machines*. New York: Wiley, 1951, p. 213.

Z. Deng, for biography see page 136 of the March 1986 issue of this TRANSACTIONS.

I. Boldea (SM'83), for biography see page 136 of the March 1986 issue of this TRANSACTIONS.

S. A. Nasar (F'85), for biography see page 136 of the March 1986 issue of this TRANSACTIONS.